From spiral growth to kinetic roughening in molecular-beam epitaxy of GaN(0001)

S. Vézian,* F. Natali, F. Semond, and J. Massies
Centre de Recherche sur l'Hétéro-Epitaxie et ses Applications, Centre National de la Recherche Scientifique, Rue B. Gregory, Sophia Antipolis, F-06560 Valbonne, France

(Received 3 September 2003; revised manuscript received 13 November 2003; published 19 March 2004)

Surface roughening of GaN layers grown by molecular-beam epitaxy using NH_3 as a nitrogen source on Si(111) substrates has been studied by *ex situ* atomic force microscopy. Mound formation is observed and analyzed using scaling concepts. The surface roughness evolution as a function of the growth time exhibits two distinct behaviors. Above a certain thickness, the growth leads to a kinetic roughening characterized by the roughness exponent $\alpha \approx 0.92$ and the dynamic exponent $\beta \approx 0.3$. However, in the first stages of the heteroepitaxial growth, a coarsening of the mounds without an increase of the roughness is observed. This behavior is inconsistent with the scaling relationship of the surface width predicted by most kinetic roughening models. Results are interpreted considering a crossover between screw dislocation induced spiral growth and kinetic roughening.

DOI: 10.1103/PhysRevB.69.125329 PACS number(s): 68.35.Ct, 81.05.Ea, 81.15.Hi, 68.37.Ps

I. INTRODUCTION

The industrial fabrication of blue and green wurtzite GaN-based light emitting diodes (LEDs) and violet laser diodes is probably the most important success story of the last ten years in the field of semiconductor material science application.[1] This is mainly due to the continuous improvement of the epitaxial growth of GaN. Even if low defect density bulk GaN substrates are still not commercially available, the optimization of the heteroepitaxial growth process on various substrates including $Al_2O_3(0001)$, SiC(0001), and Si(111) has given rise to a material quality suitable for both optoelectronic and high-power high-frequency device applications. However, the present state of knowledge of the epitaxial growth mechanisms on such highly mismatched substrates is far from the one we have on classical III-V semiconductors, such as GaAs or InP, for which very high-quality bulk substrates are used. A case in point, and one which we want to address in this paper, is the relationship between the growth mechanism and the surface morphology of heteroepitaxially grown GaN. Indeed, the (various) morphologies observed markedly differ from the one commonly obtained under usual growth conditions on homoepitaxially grown GaAs. Obviously, this can be simply related to the lattice mismatch and correlated dislocation formation inherently associated with the heteroepitaxial growth of GaN. As a matter of fact, spiral growth linked with the emergence of screw-type dislocations at the GaN(0001) surface has often been reported (see, for example, Refs. 2–4). This is well explained by the classical model of Burton, Cabrera, and Frank (BCF).[5] However, this simple picture alone is not sufficient to account for the morphology pattern evolution with growth time as well as for the key influence of the growth conditions on the pattern formation.

In the present paper, we restricted ourselves to the phenomenological study of the morphology pattern evolution as a function of the GaN thickness in the specific case of the growth on Si(111) substrate by molecular-beam epitaxy (MBE) using ammonia as the nitrogen source. However, the GaN growth conditions used, which have previously been optimized to get an overall material quality suitable for device application, are the same as those we use for the MBE growth on $Al_2O_3(0001)$ or SiC(0001). Actually, the growth induced surface morphology patterns under study here are in fact well representative of what is usually observed for GaN grown by NH_3-based MBE process.

II. EXPERIMENTS

The samples were grown by MBE using ammonia as a nitrogen precursor. Two inch Si(111) substrates with a nominal orientation were used. Prior to the growth of a thick GaN layer, a structure composed of successive epitaxial layers (AlN 40 nm/GaN 250 nm/AlN 250 nm) was grown at 920 °C for AlN and 800 °C for GaN. This type of growth procedure[6,7] has been developed in order to overcome the formation of cracks, which are due to the large difference in the thermal expansion coefficient between GaN and Si.[8] It is worth noting here that the last AlN layer on which GaN is grown is almost fully relaxed (i.e. it has its bulk parameters). All GaN layers studied in the following were grown on such a buffer layer at 800 °C (1073 K) using a NH_3 beam equivalent pressure (BEP) of 5×10^{-5} Torr and a Ga flux (BEP of 2×10^{-6} Torr) which leads to a growth rate of 1 μm/h. More details concerning the growth conditions and the material assessment can be found elsewhere.[7] It should be emphasized that the growth conditions used here and described in Ref. 7 have been optimized to get the best structural, optical, and electrical properties of GaN heteroepitaxially grown on Si(111). Such growth conditions are, for example, used to grow structures for high-power high-electron mobility transistor applications.[9] The thickness of the GaN layers, ranging from 0.2 to 3 μm, were measured using both *in situ* reflectivity and *ex situ* thin film interference. The strain state of these films was determined at the growth temperature using *in situ* reflection high-energy electron diffraction (RHEED). Tapping-mode atomic force microscopy (AFM) was used to analyze the surface morphology.

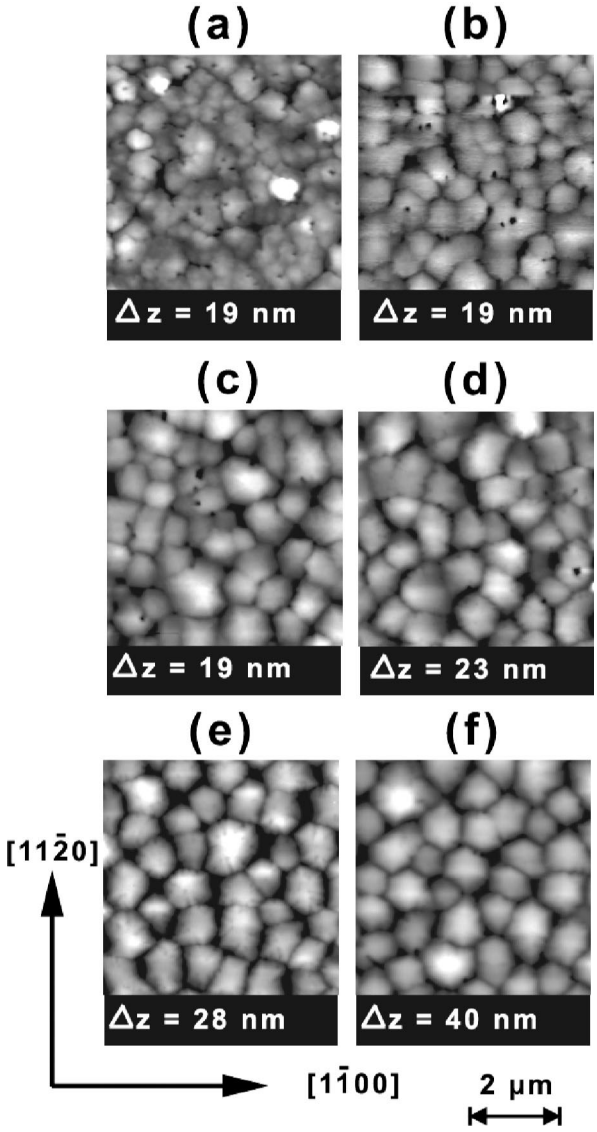

FIG. 1. 5×5-μm^2 AFM pictures of GaN films grown under the same conditions (at 1073 K with a growth rate of 1 μm/h and under excess of NH_3) but with different thickness t: (a) 0.2 μm, (b) 0.4 μm, (c) 0.65 μm, (d) 0.7 μm, (e) 2 μm, and (f) 3 μm. Δz is the gray scale value.

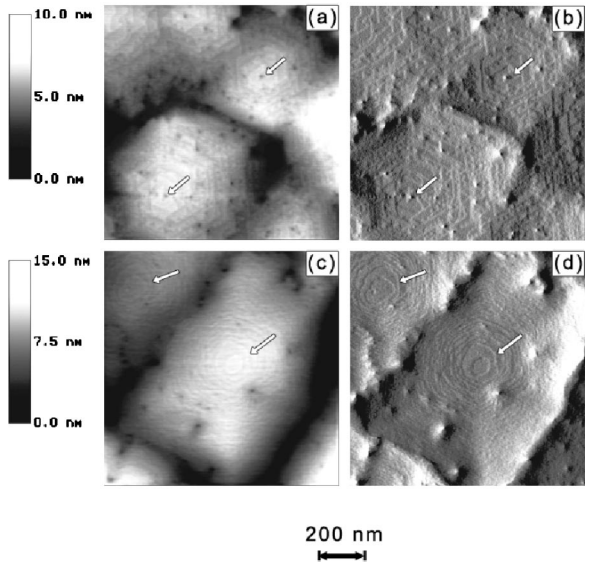

FIG. 2. 1×1-μm^2 AFM pictures of GaN films with thickness t of 0.4 μm [(a) and (b)] and 2 μm [(c) and (d)]. Note that (a) and (c) correspond to topographic mode while (b) and (d) are taken in derivative mode. White arrows indicate the location of the tops of the mounds.

III. RESULTS AND DISCUSSION

Typical AFM images of GaN layers grown with different thicknesses are presented in Fig. 1. Before describing the main morphological features, let us first briefly discuss the presence of holes with a diameter of 100–200 nm which can be noted on the AFM pictures (small black spots). These depressions are most probably associated to the mergence of nanopipes because of the high depth value measured in section profiles of the AFM data (a value of about 40 nm is found, but is clearly underestimated because of the convolution of the tip with the ledges of the hole). These holes are observed for thicknesses up to 0.7 μm with a density decreasing from 2.2×10^8 to 2.8×10^7 cm^{-2} [Figs. 1(a)–1(d)]. Such holes are commonly observed in the first stages of the heteroepitaxial growth of GaN whatever the growth method and the substrate used[10,11] and they do not play a significant role in the large scale morphology of the surface. Therefore they will not be discussed further in the following. Coming back to the main feature of the AFM pictures, we can say that all samples exhibit the same surface morphology composed of growth mounds. At first sight, they seem to be very similar to the mounds resulting from kinetic roughening, which typically occur when the growth proceeds by two-dimensional nucleation (see, for example, Ref. 12). However, higher magnification AFM pictures (Fig. 2) indicate that the mounds observed at low GaN thickness (t) present a screw-type dislocation at their tops [Figs. 2(a) and 2(b)], while it is not the case for mounds corresponding to high t [Figs. 2(c) and 2(d)]. The situation also appears more complex when analyzing the variation with growth time of both the average mound separation distance (d) obtained from the first maximum in the height-height correlation function $\langle h_i h_j \rangle$[13–15] and the surface width or roughness (w) defined as the average root-mean-square fluctuation of the mounds in ''height'' along the growth direction. We observe that d increases with the thickness (t) of the GaN film and indeed the AFM pictures [Figs. 1(a) and 1(f)] corresponding to the extreme values of t (0.2 and 3 μm) appear very different. In the early stage of the growth, the distribution of the lateral mound size is inhomogeneous and ranges from 250 to 850 nm at a layer thickness of 0.2 μm [Fig. 1(a)]. In Figs. 1(b) and 1(c) the coarsening process is clearly visible, and in the latest image the lateral mound size is ranging from 580 to 1400 nm. After an initial transient period, the surface reaches a steady state in which the density of mounds and their size do not change significantly. In Figs. 1(d)–1(f), corresponding to the thicker GaN layers (0.7–3 μm), mounds have an homogeneous size distribution and a lateral size of about 1 μm. The gray scale amplitude along the growth direction of the

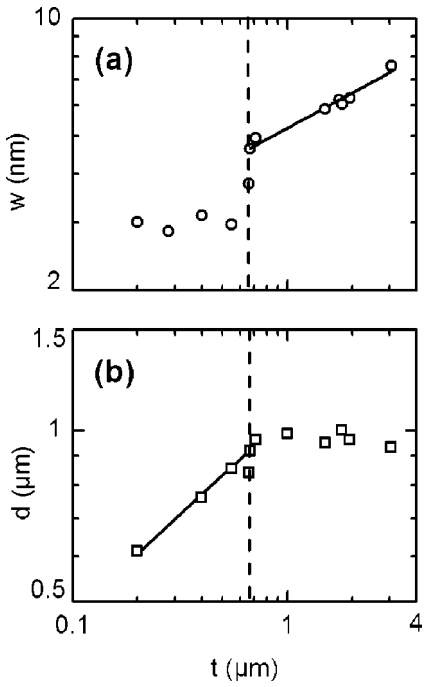

FIG. 3. Log-log plot of (a) the surface width w and (b) the average mounds separation d versus the thickness t of the GaN films. The dashed line ($t \approx 0.7\ \mu$m) highlights the boundary of the two regimes: coarsening (left) and steepening (right).

AFM pictures (Δz) increases continuously with t (see the lower panel of each AFM images shown in Fig. 1). Δz is approximately proportional to the surface width,[16] and therefore the surface width increases with the thickness of the growing GaN layer. This behavior is by definition a characteristic feature of a kinetic roughening phenomenon. Mound formation has already been reported during the growth of AlN on $Al_2O_3(0001)$ and GaN on GaN(0001).[17,18] In these two cases, the surface roughness increases and the lateral mound size coarsens with time, in good agreement with the present observation.

One possibility to better quantify the surface roughness is to calculate from the AFM topographic images the surface width $w \equiv \langle (h_i - \langle h \rangle)^2 \rangle^{1/2}$ where h_i is the film thickness at a position i of the surface and $\langle\ \rangle$ denotes an average over the growth plane. If the surface width has a scaling behavior[19] (i.e., the surface fluctuations exhibit a universal behavior) then $w(t)$ is expected to be of the form $w \propto t^{\beta}$ for small t and $w \propto L^{\alpha}$ for large t where L is the size of the region over which w is measured (α and β are respectively the roughness and the dynamic exponents where $0 < \alpha, \beta < 1$).[20,21] Figure 3(a) shows the surface width w as a function of the GaN layer thickness t calculated from several AFM images of $15 \times 15\ \mu m^2$. In this graph two growth regimes, with a transition at $t \approx 0.7\ \mu$m (indicated by the dashed line), are clearly visible. In the regime corresponding to $t > 0.7\ \mu$m, the surface width follows a power law $w \propto t^{\beta}$, where $\beta = 0.30 \pm 0.02$, in agreement with the scaling hypothesis. The dynamic exponent β physically indicates the rate of development of the roughness. Note that Tarsa *et al.*[18] reported $\beta \approx 0.5$ for the homoepitaxial growth of GaN by plasma assisted MBE under N-rich conditions. This result indicates that in their growth experiments the roughness develops faster due to the different growth conditions used, presumably leading to a lower surface diffusion.

In the first regime of growth ($t < 0.7\ \mu$m), which corresponds to the first step of the epitaxial growth of GaN onto AlN, the surface width is independent of the GaN thickness and remains constant ($w \approx 2.9$ nm). The dynamic scaling hypothesis does not predict such a result: w should obey a power law for small t. A similar behavior has been reported during the growth of fully strained $Ge_{1-x}Sn_x$ alloys on Ge(001), and interpreted as a crossover between strain-induced roughening and kinetic roughening.[22] The possible role of the strain-induced roughening (Asaro-Tiller-Grinfeld instability[23–25]) in our experiments will be discussed below.

As for the surface width, the time dependence of the average mound separation distance d exhibits two distinct regimes with a transition at the same thickness value ($t \approx 0.7\ \mu$m) [Fig. 3(b)]. In the first time segment, a coarsening behavior is observed: the relationship between d and t follows a power law dependence $d \propto t^n$ with $n = 0.35 \pm 0.03$. For comparison, exponent values of ≈ 0.7 and ≈ 0.4 have been reported during low-temperature homoepitaxy of Si and Ge, respectively.[13,14] In the second time segment, the average mound separation does not depend on t and saturates at $d \approx 0.96\ \mu$m. Seeing that $w \ll d$, the mean slope of the mounds is given in first approximation by w/d and increases with time as t^{β}. This result is however not in agreement with theoretical studies such as, for example, those of Smilauer and Vvedensky[15] and Golubovic,[26] which predict that the lateral mound size coarsens and the surface width increases at the same time.

Another possibility to quantify the surface roughness is to calculate the height difference correlation function $G(\rho) \equiv \langle (h_j - h_i)^2 \rangle$ where $h_{i,j}$ is the thickness layer at the positions i and j separated by the distance ρ in the growth plane and $\langle\ \rangle$ is an average over the different possible pairs. In this case, the scaling hypothesis states $G(\rho) \propto \rho^{2\alpha}$ for small ρ and $G(\rho) \propto t^{2\beta}$ for large ρ.[20,21] If the surface width follows the scaling relationship, then $G(\rho \to \infty)$ is directly proportional to w^2. Figure 4 shows the root height difference correlation function calculated for different thicknesses and from several AFM images. In all cases, $[G(\rho)]^{1/2}$ exhibits the scaling relationship described above. In the coarsening regime ($t < 0.7\ \mu$m) [Fig. 4(a)], we find that α increases continuously with t (0.72 at 0.2 μm, 0.78 at 0.4 μm and 0.83 at 0.55 μm). However, in the steepening regime observed for $t > 0.7\ \mu$m [Fig. 4(b)], $\alpha = 0.92 \pm 0.02$ independently of t. Physically, α is a measure of how well the roughness can be described by a single lateral length scale (for $\alpha = 1$ the scale transformation is isotropic and the surface is self-similar[21]). Thus for $t > 0.7\ \mu$m, the surface has a well defined scaling behavior with $\alpha = 0.92$ and $\beta = 0.3$.[27] This behavior is therefore very different from the one observed for $t < 0.7\ \mu$m, where the surface pattern is highly dependent of the deposit thickness and evolves during time.

The kinetic origin of the pattern observed for $t > 0.7\ \mu$m can be confirmed by annealing experiments. Figure 5(a)

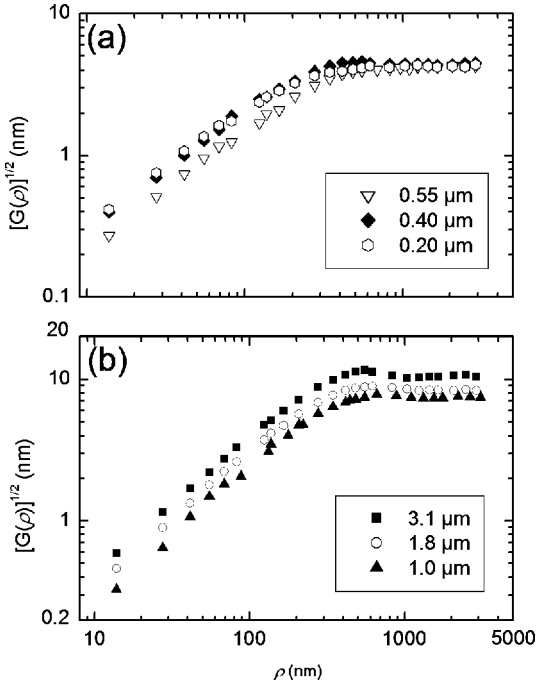

FIG. 4. Log-log plot of the root height difference correlation function $[G(\rho)]^{1/2}$ of surface points separated by a distance ρ for samples in the coarsening (a) and in the steepening (b) surface evolution modes.

shows the surface morphology obtained after thermal annealing of a 2-μm-thick GaN sample grown using the conditions described in Sec. II. Annealings have been carried out in a commercial metalorganic vapor phase epitaxy (MOVPE) system (Thomas Swan Scientific Equipment) during 15 min at 1000 °C (1273 K) and under an ammonia pressure of 100 Torr. Compared to AFM images shown in Fig. 1, the morphology has drastically changed. The surface exhibits large flat terraces with a molecular step height (2.59 Å), and the surface width w calculated from 15×15 μm^2 AFM pictures is also lower (1 nm). The morphology is in fact very similar to the one observed for surfaces of GaN grown by the MOVPE method,[3] for which the growth temperature ranges from 1000 to 1100 °C. This experiment thus provides further evidence of the kinetic origin of the surface roughening observed during the MBE growth of thick GaN layers: the surfaces obtained by high-temperature annealing of such MBE grown layers are closer to the equilibrium than as grown layers the resulting morphology being imposed only by the initial residual tilt of the substrate and step pinning by screw-type dislocations.[28] This can clearly be seen in Fig. 5(b), which is a high magnification AFM picture of a surface obtained by thermal annealing. In this 1×1-μm^2 picture, the presence of small pits or depressions is associated with the emergence of threading dislocations.[3,29] Depressions linked to two (or a multiple of two) molecular step edges are associated with screw-type dislocations [see the white arrows in Fig. 5(b)], while the other are connected to edge-type dislocations located at the crystallographic subgrain boundaries.[29]

Coming back now to the first regime of growth (t

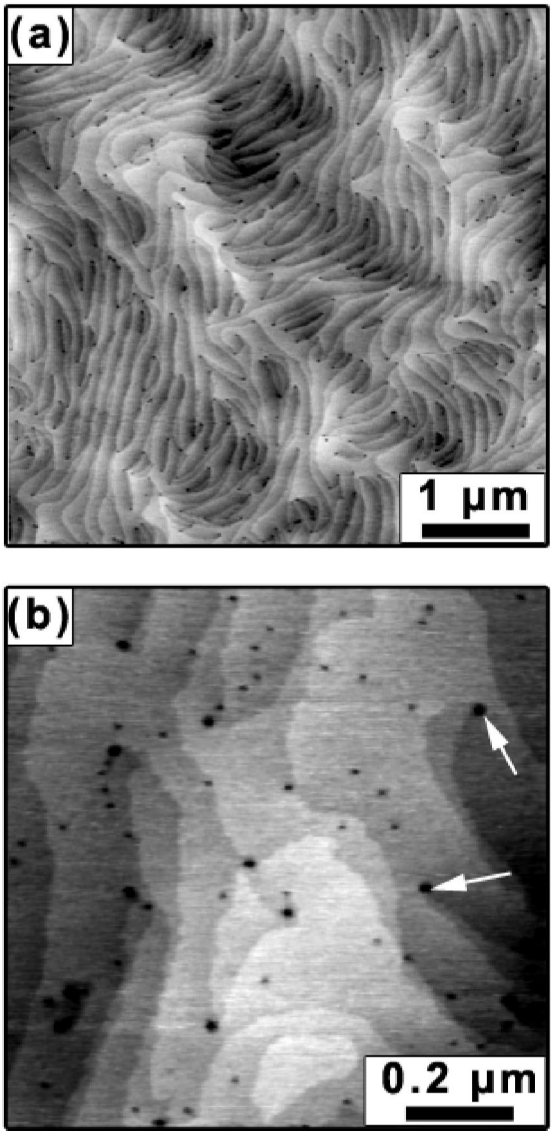

FIG. 5. AFM pictures of 2-μm-thick MBE-grown GaN sample after an annealing treatment of 15 min at 1273 K and under a NH_3 pressure of 100 Torr performed in a MOVPE reactor. (a) 5×5 μm^2 (b) 1×1 μm^2 zoom ins. Small pits are associated with edge dislocations and large pits with screw dislocations (white arrows). Before annealing the surface morphology is identical to the one corresponding to Fig. 1(e).

<0.7 μm) and remembering that the growth occurs on a relaxed AlN buffer layer, it can be put forward that the lattice mismatch induced strain plays a key role in the morphology pattern formation and evolution. Elastic strain relaxation through strain-induced roughening (Asaro-Tiller-Grinfeld instability) is indeed well known to markedly affect the planarity of the surface by giving rise to a surface undulation. The associated wavelength can be given by $\lambda=[\pi\gamma(1-\nu)]/[2\mu\varepsilon^2(1+\nu)^2]$, where μ and ν are the film shear modulus and Poisson ratio, γ is the surface energy, and ε is the misfit strain between the film and the substrate.[22,30] The material constants for GaN, $\mu=125$ GPa and $\nu=0.21$, are calculated with the stiffness coefficients C_{ij} given in Ref. 31. Considering that the growth of GaN is performed under

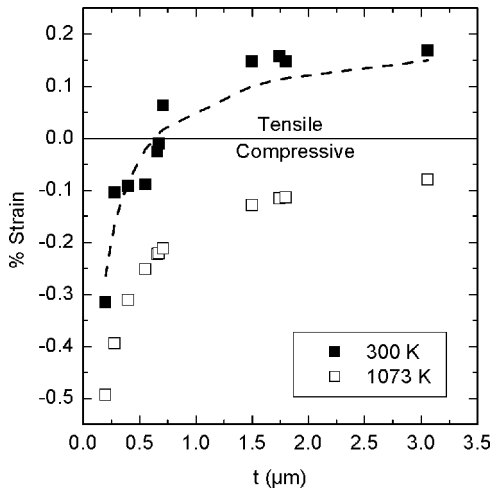

FIG. 6. Growth temperature (open symbols) and room temperature (solid symbols) residual strain vs GaN thickness t. Data are respectively calculated from lattice mismatch variation recording *in situ* by RHEED and from *ex situ* photoluminescence and reflectivity measurements at 10 K (see the text). The dashed line corresponds to the variation of the strain state calculated by adding a constant tensile strain (due to the sample cooling) to values at growth temperature (see the text).

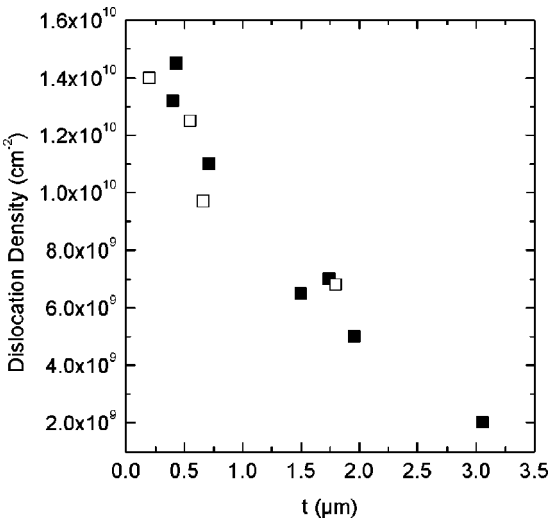

FIG. 7. Total threading dislocation density versus GaN thickness. Data are obtained both by AFM (solid symbols) and TEM (open symbols) measurements.

N-rich conditions, γ could be approximated[32] by 185 meV/Å^2. The lattice mismatch between AlN and GaN is 2.5%, and therefore we find $\lambda \approx 50$ nm. This value is largely smaller than the surface periodicity measured in our samples [see the d values in Fig. 3(b)]. Note however that such estimation of λ can be meaningful only for coherent growth, which is not the case here as we will see below.

In order to further investigate the relationship between the surface behavior observed at $t < 0.7$ μm and the actual strain in the epitaxial layer, we have evaluated the strain state of our samples as a function of GaN thickness both at growth temperature (1073 K) and at room temperature. Figure 6 shows the in-plane deformation at 1073 K (open symbols) calculated from the in-plane lattice parameter variation recorded in real time during the growth by RHEED (see, for example, Ref. 33). Values at 300 K (solid symbols) are deduced from low-temperature (10 K) photoluminescence and reflectivity measurements.[34–37] About 4/5 of the initial strain resulting from the lattice mismatch between AlN and GaN (2.5%) is relaxed within the first 0.2 μm of GaN growth. The remaining 0.5% compressive residual strain is then relaxed over the next 3 μm of growth. When the sample is cooling after the growth, a tensile component is added to the strain. Assuming that between 300 and 1073 K the thermal expansion coefficients of GaN and Si can be considered constant, then the thermal tensile strain is $(\alpha_{\mathrm{GaN}}\text{-}\alpha_{\mathrm{Si}}) \times \Delta T = 0.23\%$ with $\alpha_{\mathrm{GaN}} = 5.59 \times 10^{-6}$ K^{-1} and $\alpha_{\mathrm{Si}} = 2.59 \times 10^{-6}$ K^{-1}.[38,39] Actually, adding a constant tensile value of 0.23% (dashed line in Fig. 6) to data measured at 1073 K give a reasonable agreement with our room temperature data (solid symbols).

A question which remains is how the strain is relaxed. We know, from our own experience and a large body of published results, that strain relaxation of GaN on a relaxed AlN buffer layer occurs by the formation of threading dislocations from the very beginning of the growth (the critical thickness for plastic relaxation is about 30 Å; see, for example, Ref. 40). However, to get more insight into the strain relaxation of the layers studied in the present work, we have determined the dislocation density as a function of the GaN thickness. The dislocation density in epitaxial layers can be classically deduced from plan-view transmission electron microscopy (TEM) observations. It is now also well established that dislocation density can be more simply obtained from near-field microscopy pictures such as the one given in Fig. 5(b).[29,41] Actually, we have used both methods. Figure 7 shows the dislocation density measured for different GaN thicknesses using both AFM (solid symbols) and TEM (open symbols). We find a good agreement between values obtained with the two independent techniques. The dislocation density exponentially decreases with the film thickness, which emphasizes the origin of the strain relaxation. Sahonta *et al.* have observed that compressive strain in GaN layers is relaxed by the lateral migration of threading dislocations and their reaction to form loops.[42] On the basis of cross-section TEM observations, we also find that strain relaxation in our samples is principally due to the interaction between threading dislocations. As a conclusion, strain relaxation in our samples is mainly due to plastic relaxation by dislocation formation from the very beginning of the growth and not by elastic relaxation through Asaro-Tiller-Grinfeld instability.

Therefore we should think about another reason for the mound formation observed in the first stages of growth ($t < 0.7$ μm). In a previous work,[43] we have shown that the surface morphology of GaN(0001) layers grown by MBE using NH_3 is strongly dependent on the growth kinetics. Growing under N-rich or slightly Ga-rich conditions changes not only the morphological pattern but also the roughness evolution as the growth proceeds. Slightly Ga-rich growth conditions give rise to spiral growth, as predicted by the BCF theory for step-flow growth in presence of screw dislocations.[5] In this case, the surface width is independent of the film thickness.[43] Actually, this surface behavior is very

similar to the one observed in the present N-rich growth conditions at $t<0.7\ \mu$m as Figs. 2(a), 2(b) and 3(a) show, although a growth mode where two-dimensional (2D) nucleation is active is suggested by the kinetic roughening which occurs at large thickness. To understand this apparent contradiction, one has to consider the effect of strain on surface diffusion. As experimentally shown in the system Ag on Pt(111) by Brune *et al.*[44] and theoretically predicted (for example by Schroeder and Wolf[45]), compressive strain enhances surface diffusion. Also, a theoretical study by Ratsch and Zangwill[46] indicated that step-flow growth is obtained at lower temperature in the presence of strain.

The above ideas can be assembled to tentatively propose a growth mechanism scenario leading to the breakdown observed in the surface width evolution at $t\approx0.7\ \mu$m. In the first stage of strained epitaxy of GaN on AlN, a high density dislocation network is rapidly formed and surface diffusion is sufficient to allow screw dislocation mediated step-flow growth via the BCF mechanism. The surface pattern is thus formed by growth spirals initiated by dislocations with a screw component. As the thickness increases, the misfit strain relaxes via the interaction between dislocations (formation of loops).[42] As a consequence, the dislocation density decreases, which in turn implies that the density of ''mounds'' (in this case growth spirals) also decreases. Thus the growth spirals coarsen while the surface width remains constant. A similar GaN growth morphology behavior is observed[43] when the growth of (relaxed) GaN is carried out under near-stoichiometry conditions, where the surface diffusion is enhanced compared to usual growth under excess of NH_3 (also see Ref. 47). In the present case, it is suggested that surface diffusion is enhanced at the beginning of the growth by the compressive misfit strain. As the strain decreases with the film thickness, the diffusion length decreases. At a residual strain of $(-0.21\pm0.03)\%$ (see Fig. 6) the diffusion length and the terrace width become similar, leading to a transition from step-flow-dominated growth to a mixed growth mode where 2D nucleation is active. This is consistent with the fact that for growth of relaxed GaN in similar conditions, RHEED oscillations completely vanish only for a growth temperature above $\approx800\,^{\circ}$C, which indicates that 2D nucleation is active up to this temperature.[33]

IV. CONCLUSION

The surface of GaN grown by MBE using ammonia onto a relaxed AlN buffer layer on Si(111) substrates has been studied by *ex situ* atomic force microscopy. Surface roughening was observed, leading to the formation of growth mounds. Scaling concepts were used to analyze the surface morphology evolution. We found two distinct behaviors depending on the GaN thickness. For thicknesses above 0.7 μm, growth gives rise to a kinetic roughening characterized by the scaling behavior of the surface. Critical exponents are well defined with $\alpha=0.92\pm0.02$ and $\beta=0.30\pm0.02$. For thicknesses up to 0.7 μm, the situation is drastically different: α increases with time and the surface roughness remains constant (i.e., $\beta=0$). Furthermore, a coarsening of the growth mounds was observed and correlated to the dislocation density decrease. It is suggested that the misfit strain due to the heteroepitaxial growth plays a key role in the crossover from screw dislocation induced spiral growth to kinetic roughening. In the first stages of growth, surface diffusion can be enhanced by the compressive strain, leading to spiral formation via a BCF mode of growth. As the growth proceeds, strain relaxation increases and correlatively the surface diffusion decreases. This leads to a transition from step-flow-dominated growth mode to a mixed growth mode where 2D nucleation is sufficiently active to give rise to kinetic roughening.

ACKNOWLEDGMENTS

The authors thankfully acknowledge M. Leroux for a critical reading of the paper. We are grateful to D.J. Byrne for thin film interference measurements. We also thank O. Tottereau and P. Vennéguès for TEM characterizations and B. Beaumont and Z. Bougrioua for MOVPE annealing experiments.

*Corresponding author. sv@crhea.cnrs.fr

[1] S. Nakamura and G. Fasol, *The Blue Laser Diode* (Springer-Verlag, Berlin, 1997).
[2] A. R. Smith, V. Ramachandran, R. M. Feenstra, D. W. Greve, M.-S. Shin, M. Skowronski, J. Neugebauer, and J. E. Northrup, J. Vac. Sci. Technol. A **16**, 1641 (1998).
[3] B. Heying, E. J. Tarsa, C. R. Elsass, P. Fini, S. P. DenBaars, and J. S. Speck, J. Appl. Phys. **85**, 6470 (1999).
[4] A. Parkhomovsky, A. M. Dabiran, B. Benjaminsson, and P. I. Cohen, Appl. Phys. Lett. **78**, 2315 (2001).
[5] W. K. Burton, N. Cabrera, and F. C. Frank, Philos. Trans. R. Soc. London, Ser. A **243**, 299 (1951).
[6] S. A. Nikishin, N. N. Faleev, V. G. Antipov, S. Francoeur, L. Grave de Peralta, G. A. Seryogin, H. Temkin, T. I. Prokofyeva, M. Holtz, and S. N. G. Chu, Appl. Phys. Lett. **75**, 2073 (1999).
[7] F. Semond, Y. Cordier, N. Grandjean, F. Natali, B. Damilano, S. Vézian, and J. Massies, Phys. Status Solidi A **188**, 501 (2001).
[8] D. M. Follstaedt, J. Han, P. Provencio, and J. G. Fleming, MRS Internet J. Nitride Semicond. Res. **4S1**, G3.72 (1999).
[9] R. Behtash, H. Tobler, M. Neuburger, A. Schurr, H. Leier, Y. Cordier, F. Semond, F. Natali, and J. Massies, Electron. Lett. **39**, 626 (2003).
[10] W. Qian, M. Skowronski, K. Doverspike, L. B. Rowland, and D. K. Gaskill, J. Cryst. Growth **151**, 396 (1995).
[11] P. Vennéguès, B. Beaumont, M. Vaille, and P. Gibart, Appl. Phys. Lett. **70**, 2434 (1997).
[12] M. D. Johnson, C. Orme, A. W. Hunt, D. Graff, J. Sudijono, L. M. Sander, and B. G. Orr, Phys. Rev. Lett. **72**, 116 (1994).
[13] N.-E. Lee, D. G. Cahill, and J. E. Greene, Phys. Rev. B **53**, 7876 (1996).
[14] J. E. Van Nostrand, S. J. Chey, M.-A. Hasan, D. G. Cahill, and J. E. Greene, Phys. Rev. Lett. **74**, 1127 (1995).
[15] P. Smilauer and D. D. Vvedensky, Phys. Rev. B **52**, 14263 (1995).
[16] Δz is chosen to be four times the standard deviation of the Gaussian distribution of height.
[17] W. Kim, M. Yeadon, A. E. Botchkarev, S. N. Mohammad, J. M.

Gibson, and H. Morkoç, J. Vac. Sci. Technol. B **15**, 921 (1997).
[18] E. J. Tarsa, B. Heying, X. H. Wu, P. Fini, S. P. DenBaars, and J. S. Speck, J. Appl. Phys. **82**, 5472 (1997).
[19] F. Family and T. Vicsek, J. Phys. A **18**, L75 (1985).
[20] A. Pimpinelli and J. Villain, *Physics of Crystal Growth* (Cambridge University Press, Cambridge, 1988).
[21] A.-L. Barabasi and H. E. Stanley, *Fractal Concepts in Surface Growth* (Cambridge University Press, Cambridge, 1995).
[22] P. Desjardins, T. Spila, O. Gurdal, N. Taylor, and J. E. Greene, Phys. Rev. B **60**, 15993 (1999).
[23] R. J. Asaro and W. A. Tiller, Metall Trans. A **3**, 1789 (1972).
[24] M. Y. Grinfeld, Dokl. Akad. Nauk SSSR **265**, 836 (1982) [Sov. Phys. Dokl. **31**, 831 (1986)].
[25] J. Villain, C. R. Physique **4**, 201 (2003).
[26] L. Golubovic, Phys. Rev. Lett. **78**, 90 (1997).
[27] Note that these critical exponents are close to those found for growth with surface diffusion ($\alpha=1$ and $\beta=1/4$) by D. E. Wolf and J. Villain, Europhys. Lett. **13**, 389 (1990).
[28] F. C. Frank, Discuss. Faraday Soc. **5**, 67 (1949).
[29] S. Vézian, J. Massies, F. Semond, N. Grandjean, and P. Vennégues, Phys. Rev. B **61**, 7618 (2000).
[30] H. Gao, J. Mech. Phys. Solids **42**, 741 (1994).
[31] A. Polian, M. Grimsditch, and I. Grzegory, J. Appl. Phys. **79**, 3343 (1996).
[32] J. Elsner, M. Haugk, G. Jungnickel, and T. Frauenheim, Solid State Commun. **106**, 739 (1998).
[33] N. Grandjean and J. Massies, Appl. Phys. Lett. **71**, 1816 (1997).
[34] Values at 300 K are deduced from low-temperature reflectivity measurements using the relation between the energy of the *A* exciton E_A and the in plane deformation ε_{xx} ($\Delta E_A/\Delta\varepsilon_{xx}=-8.5$ eV and $\varepsilon_{xx}=0$ for $E_A=3.479$ eV; see Refs. 35–37).
[35] W. Shan, R. J. Hauenstein, A. J. Fischer, J. J. Song, W. G. Perry, M. D. Bremser, R. F. Davis, and B. Goldenberg, Phys. Rev. B **54**, 13460 (1996).
[36] A. Shikanai, T. Azuhata, T. Sota, S. Chichibu, A. Kuramata, K. Horino, and S. Nakamura, J. Appl. Phys. **81**, 417 (1997).
[37] H. Lahrèche, M. Leroux, M. Laügt, M. Vaille, B. Beaumont, and P. Gibart, J. Appl. Phys. **87**, 577 (2000).
[38] H. P. Maruska and J. J. Tietjen, Appl. Phys. Lett. **15**, 327 (1969).
[39] O. Madelung, *Semiconductors* (Springer-Verlag, Berlin, 1971).
[40] B. Damilano, N. Grandjean, F. Semond, J. Massies, and M. Leroux, Appl. Phys. Lett. **75**, 962 (1999).
[41] D. Kapolneck, X. H. Wu, B. Heying, S. Keller, B. P. Keller, U. K. Mishra, S. P. DenBaars, and J. Speck, Appl. Phys. Lett. **67**, 1541 (1995).
[42] S.-L. Sahonta, M. Q Baines, D. Cherns, H. Amano, and F. A. Ponce, Phys. Status Solidi B **234**, 952 (2002).
[43] S. Vézian, J. Massies, F. Semond, and N. Grandjean, Mater. Sci. Eng., B **82**, 56 (2001).
[44] H. Brune, K. Bromann, H. Roder, K. Kern, J. Jacobsen, P. Stoltze, K. Jacobsen, and J. Norskov, Phys. Rev. B **52**, R14380 (1995).
[45] M. Shroeder and D. E. Wolf, Surf. Sci. **375**, 129 (1997).
[46] C. Ratsch and A. Zangwill, Appl. Phys. Lett. **63**, 2348 (1993).
[47] C. Adelman, J. Brault, E. Martinez-Guerrero, G. Mula, H. Mariette, Le Si Dang, and B. Daudin, Phys. Status Solidi A **188**, 575 (2001).